A Partial Loss-of-Function Variant in *AKT2* Is Associated With Reduced Insulin-Mediated Glucose Uptake in Multiple Insulin-Sensitive Tissues: A Genotype-Based Callback Positron Emission Tomography Study

Aino Latva-Rasku,[1] Miikka-Juhani Honka,[1] Alena Stančáková,[2] Heikki A. Koistinen,[3,4] Johanna Kuusisto,[2,5] Li Guan,[6] Alisa K. Manning,[7,8,9] Heather Stringham,[6] Anna L. Gloyn,[10,11,12] Cecilia M. Lindgren,[7,10,13] T2D-GENES Consortium, Francis S. Collins,[14] Karen L. Mohlke,[15] Laura J. Scott,[6] Tomi Karjalainen,[1] Lauri Nummenmaa,[1,16] Michael Boehnke,[6] Pirjo Nuutila,[1,17] and Markku Laakso[2,5]

Diabetes 2018;67:334–342 | https://doi.org/10.2337/db17-1142

Rare fully penetrant mutations in *AKT2* are an established cause of monogenic disorders of glucose metabolism. Recently, a novel partial loss-of-function *AKT2* coding variant (p.Pro50Thr) was identified that is nearly specific to Finns (frequency 1.1%), with the low-frequency allele associated with an increase in fasting plasma insulin level and risk of type 2 diabetes. The effects of the p.Pro50Thr *AKT2* variant (p.P50T/*AKT2*) on insulin-stimulated glucose uptake (GU) in the whole body and in different tissues have not previously been investigated. We identified carriers (*N* = 20) and matched noncarriers (*N* = 25) for this allele in the population-based Metabolic Syndrome in Men (METSIM) study and invited these individuals back for positron emission tomography study with [^{18}F]-fluorodeoxyglucose during euglycemic hyperinsulinemia. When we compared p.P50T/*AKT2* carriers to noncarriers, we found a 39.4% reduction in whole-body GU (*P* = 0.006) and a 55.6% increase in the rate of endogenous glucose production (*P* = 0.038). We found significant reductions in GU in multiple tissues—skeletal muscle (36.4%), liver (16.1%), brown adipose (29.7%), and bone marrow (32.9%)—and increases of 16.8–19.1% in seven tested brain regions. These data demonstrate that the p.P50T substitution of *AKT2* influences insulin-mediated GU in multiple insulin-sensitive tissues and may explain, at least in part, the increased risk of type 2 diabetes in p.P50T/*AKT2* carriers.

Many large-scale exome and genome sequencing studies currently are under way to identify low-frequency and rare genetic variants associated with human diseases and traits. Large samples typically are required to obtain convincing association evidence for such variants. Once a rare-variant association is identified, investigators may call back carriers

[1]Turku PET Centre, University of Turku, Turku, Finland
[2]Internal Medicine, Institute of Clinical Medicine, University of Eastern Finland, Kuopio, Finland
[3]University of Helsinki and Department of Medicine, Helsinki University Central Hospital, Helsinki, Finland
[4]Minerva Foundation Institute for Medical Research, Helsinki, Finland
[5]Department of Medicine, Kuopio University Hospital, Kuopio, Finland
[6]Department of Biostatistics and Center for Statistical Genetics, University of Michigan, Ann Arbor, MI
[7]Program in Medical and Population Genetics, Broad Institute, Cambridge, MA
[8]Clinical and Translational Epidemiology Unit, Massachusetts General Hospital, Boston, MA
[9]Department of Medicine, Harvard Medical School, Boston, MA
[10]Wellcome Trust Centre for Human Genetics, Nuffield Department of Medicine, University of Oxford, Oxford, U.K.
[11]Oxford Centre for Diabetes, Endocrinology and Metabolism, Radcliffe Department of Medicine, University of Oxford, Oxford, U.K.
[12]National Institute for Health Research Oxford Biomedical Research Centre, Oxford University Hospitals NHS Foundation Trust, Oxford, U.K.
[13]Big Data Institute, Li Ka Shing Centre for Health Information and Discovery, University of Oxford, Oxford, U.K.
[14]National Human Genome Research Institute, National Institutes of Health, Bethesda, MD
[15]Department of Genetics, University of North Carolina at Chapel Hill, Chapel Hill, NC
[16]Department of Psychology, University of Turku, Finland
[17]Department of Endocrinology, Turku University Hospital, Turku, Finland

Corresponding authors: Markku Laakso, markku.laakso@uef.fi, Pirjo Nuutila, pirjo.nuutila@utu.fi, and Michael Boehnke, boehnke@umich.edu.

Received 21 September 2017 and accepted 7 November 2017.

M.B., P.N., and M.L. shared last authorship.

and noncarriers of the associated variant from the study population and undertake additional phenotyping to help understand disease mechanism. Such phenotyping might not have been considered at study outset or might have been too costly to undertake in the full study sample. Finland provides an ideal base for genotype callback studies. The history of Finland, with recent population bottlenecks, has resulted in increased frequency of genetic variants that are rare elsewhere, including nonsynonymous and particularly loss-of-function variants (1). Further, Finland boasts a well-educated population strongly supportive of biomedical research. In our present study we applied this callback approach to investigate the effects of a partial loss-of-function variant p.Pro50Thr (rs184042322) *AKT2* (V-AKT Murine Thymoma Viral Oncogene Homolog 2) (p.P50T/*AKT2*) on the rates of glucose uptake (GU) in whole body and in multiple insulin-sensitive tissues to understand the mechanisms explaining increased risk of type 2 diabetes in p.P50T/*AKT2* carriers.

The AKT2 protein plays a key role in the conserved phosphoinositide 3-kinase signaling pathway, downstream of the insulin receptor, and mediates the physiological effects of insulin in several tissues including liver, skeletal muscle, and adipose tissue (2–4). Additionally, *AKT2* is expressed in the bone marrow, heart, brain, small intestine, and kidney. Mice deficient in Akt2 develop hyperglycemia, hyperinsulinemia, insulin resistance, age-dependent loss of adipose tissue, and diabetes in males (1,5).

In humans, rare penetrant mutations in the *AKT2* gene encoding AKT serine/threonine kinase 2 have been previously associated with monogenic disorders of glucose metabolism. The first p.Arg274His mutation described in a single family showed autosomal dominant inheritance of severe insulin resistance and diabetes and disrupted insulin signaling in cultured cells. Individuals with this loss-of-function mutation were unable to phosphorylate glycogen synthase kinase 3 (GSK3) in an in vitro kinase assay (6). In contrast, another mutation, p.Glu17Lys, caused severe fasting hypoinsulinemic hypoglycemia. AKT2 p.Glu17Lys was constitutively located at the plasma membrane (7) and overexpression induced translocation of glucose transporter type 4 (GLUT4) to the plasma membrane (8).

In a recent meta-analysis of exome genotype data on 33,231 individuals of European ancestry without diabetes, investigators demonstrated that carriers of the low-frequency amino acid substitution p.P50T/*AKT2* had on average a 12% (95% CI 7–18%, $P = 1.0 \times 10^{-9}$) increase in fasting insulin level and an increased risk of type 2 diabetes (allele-specific odds ratio 1.05, $P = 8.1 \times 10^{-5}$) (9). In vitro studies demonstrated the variant protein leads to a partial loss of AKT2 phosphorylation at its activation sites (Thr308 and Ser473), suggesting impaired AKT2 signaling and a reduced ability to phosphorylate its downstream target GSK3β (9). The p.P50T/*AKT2* variant was found at a frequency of 1.1% in Finns, but it was present at much lower frequencies in other ancestries (minor allele frequency 0.2% in non-Finnish Europeans and ≤0.01% in African American, Asian, and Hispanic individuals), making Finland the ideal place for more detailed genotype-phenotype investigations.

RESEARCH DESIGN AND METHODS

The METSIM Positron Emission Tomography Studies

Study Participants

We selected male participants from the ongoing Metabolic Syndrome in Men (METSIM) follow-up study with (N = 20, 1 homozygous, 19 heterozygous) and without (N = 25) p.P50T/*AKT2* and matched for age and BMI (10,11). They fulfilled the following inclusion criteria: age 50–75 years, BMI 20–40 kg/m^2, and an oral glucose tolerance test not indicating diabetes. We applied the following exclusion criteria: diabetes, a chronic disease that could affect glucose metabolism (e.g., liver, kidney, thyroid, cancer), abusive use of alcohol, and any chronic medication that could affect glucose metabolism (e.g., steroids, β-blockers, thiazide diuretics, antipsychotics, antidepressants). We performed positron emission tomography (PET) studies at the PET Centre of the University of Turku, Finland. Assuming the sample sizes of 20 and 25 in the two groups, we had 80% power at significance level $\alpha = 0.05$ to detect a 30% difference in the means of skeletal muscle GU based on previous studies performed at the Centre. The Ethics Committee of the Hospital District of Southwest Finland approved the study protocol. The study was conducted according to the principles of the Declaration of Helsinki. All participants gave written informed consent prior to participation in the study.

Genotyping

We originally genotyped the participants of the METSIM study on the Illumina HumanExome Beadchip (9). We confirmed the p.P50T/*AKT2* genotypes with TaqMan Allelic Discrimination Assays (Applied Biosystems) for PET study participants.

Hyperinsulinemic-Euglycemic Clamp

We performed a hyperinsulinemic-euglycemic clamp after an overnight fast of 10–12 h. Two catheters were inserted in veins of opposite forearms: one in the right antecubital vein for blood sampling and another in the left forearm for glucose and insulin infusions and radiotracer injection. To obtain arterialized venous plasma, the right arm was warmed. After catheterization, we collected baseline samples and performed the hyperinsulinemic-euglycemic clamp as previously described (12) with the insulin infusion rate of 40 mU/m^2 body surface area/min (Actrapid; Novo Nordisk, Copenhagen, Denmark). We maintained euglycemia by moderating the rate of 20% glucose infusion based on the plasma glucose level measured every 5–10 min. We reported the rates of whole-body GU (M value) as the average of 20-min intervals between 60–140 min after the start of insulin infusion.

GU Measurements Using PET/CT During the Hyperinsulinemic-Euglycemic Clamp

We quantified the rates of tissue-specific GU using the PET/CT (Discovery 690; GE Medical Systems, Milwaukee, WI), with 2-deoxy-2-[^{18}F]fluoro-D-glucose (^{18}F-FDG) as tracer.

The method of producing the tracer has been previously described (13). After reaching a steady euglycemia (69 ± 15 min from the start of insulin infusion), we injected participants with 152 ± 10 MBq of ^{18}F-FDG and started PET scanning. The scanned regions were heart (40 min), liver (15 min), upper abdomen (15 min), thigh skeletal muscle (15 min), neck (10 min), and brain (10 min). We performed all PET measurements blinded to *AKT2* genotype.

Endogenous Glucose Production

We collected a urine sample immediately after GU measurements and measured the amount of radiotracer lost into urine using an isotope dose calibrator (Model VDC-205; Comecer Netherlands, Joure, Netherlands). We assessed endogenous glucose production (EGP) by subtracting glucose infusion rate from rate of glucose disposal derived from ^{18}F-FDG consumption (14). The liver produces ~80% of EGP and the kidney ~20% (15).

Nonbrain PET GU

Before analysis, we corrected imaging data for dead time, decay, and photon attenuation. To determine the input function, we calculated a blood time-activity curve by combining arterial blood activity data from the PET images (first 10 min after injection) with measurements made from arterialized venous blood plasma samples collected at nine time points (5, 10, 20, 30, 40, 47.5, 62.5, 75, and 85 min after injection) during the scanning (16). We determined plasma activity using an automatic gamma counter (Wizard 1480 3; Wallac, Turku, Finland). We derived tissue activity and fractional uptake (K_i) of the tracer from graphical analyses (17) applying the Carimas Software (version 2.9, Turku PET Centre, downloadable at http://www.turkupetcentre.fi/software/). We used a segmenting tool for myocardium to include the left ventricle wall and septum in the analysis; for other tissues the regions of interest (ROIs) were drawn manually. For skeletal muscle analysis, ROIs were drawn to include the medial parts of quadriceps femoris muscle of both thighs; for the liver, a section of the right lobe free of large vessels was chosen. The same researcher (A.L.-R.) performed analyses blinded and estimated the rates of skeletal muscle and liver GU twice for the first 24 participants. The Pearson correlation between the two measurements was 0.99 for skeletal muscle and 0.92 for liver.

We report the average of several ROIs for different adipose tissue types, with subcutaneous adipose tissue ROIs positioned around waistline, visceral adipose tissue ROIs in intraperitoneal cavity, and brown adipose tissue ROIs in supraclavicular areas on both sides of the neck. Bone marrow ROIs were drawn inside the body of both femoral bones and reported as their average.

Brain PET GU

We carried out preprocessing and statistical analyses of the brain PET images with the SPM 12 software (http://www.fil.ion.ucl.ac.uk/spm/). We first normalized PET images into an in-house ^{18}F-FDG template according to the Montreal Neurological Institute standard using linear and nonlinear transformations and smoothed with a Gaussian kernel with 8-mm full width at half maximum. Next, we quantified the voxelwise fractional uptake rate as the ratio of tissue time activity and integral of plasma activity from time 0 to the time of the scan. We compared voxelwise between-group differences in fractional uptake rate using a nonparametric full-volume analysis in the SnPM13 toolbox (http://warwick.ac.uk/snpm). We constructed anatomical ROIs in the brain lobes, midbrain, limbic system, and cerebellum in a manner parallel to that for the other tissues.

Calculation of Tissue-Specific GU

To assess the rates of tissue-specific GU (μmol/kg/min), we multipled tissue fractional uptake by plasma glucose concentration during scanning and divided by tissue density and a previously established lumped constant: 1.2 for skeletal muscle, 1.0 for myocardium and liver, 1.14 for adipose tissue, 1.1 for intestine, and 0.65 for brain (18–24). The lumped constant for bone marrow has not been defined, so we adopted the previously used value of 1.0 (25) to compare the results between groups.

Laboratory Measurements

We measured plasma glucose in duplicates using the glucose oxidase method (Analox GM9; Analox Instruments, London, UK) in the fasting state and during the clamp. We determined plasma insulin levels in the fasting state and at 30-min intervals after the start of insulin infusion until the end of clamp using an automated electrochemiluminescence immunoassay (Cobas 8000; Roche Diagnostics, Mannheim, Germany). We measured serum free fatty acid (FFA) levels in the fasting state and at 60-min intervals during the clamp with an enzymatic colorimetric method assay (NEFA-HR2, ACS-ACOD; Wako Chemicals, Neuss, Germany; Cobas 8000 c502 Analyzer, Roche Diagnostics).

Statistical Analyses

We carried out data analyses with IBM SPSS 21.0 for Windows (Chicago, IL). We give the results for continuous variables as means ± SD. We logarithm transformed variables with skewed distribution (insulin, triacylglycerol, FFA, GU in subcutaneous and visceral adipose tissue) prior to statistical analyses. We assessed the differences between the groups by the independent samples *t* test for continuous variables and χ^2 test for discrete variables. We used linear regression to adjust the results for outside temperature in the previous 30, 14, and 7 days in statistical analyses of brown adipose tissue GU. We assessed the correlation between different measures of GU by the Spearman correlation coefficient. We used the Fisher *r*-to-*z* transformation to compare correlation coefficients in carriers and noncarriers of the p.P50T/*AKT2*. The threshold for statistical significance was set at $\alpha = 0.05$.

RESULTS

The Euglycemic-Hyperinsulinemic Clamp and PET Study

Characteristics of the Participants

Characteristics of the p.P50T/*AKT2* carriers ($N = 20$, 1 homozygous, 19 heterozygous) and noncarriers ($N = 25$) without

chronic diseases are presented in Table 1. These two groups of participants were matched for age and BMI and did not differ significantly by age, BMI, or fasting glucose. As expected, fasting insulin was higher in the p.P50T/*AKT2* carriers than in the noncarriers. We pooled the single p.P50T/*AKT2* homozygous carrier with heterozygous carriers in all statistical analysis because the homozygous carrier was not an outlier among the group of carriers.

Whole-Body GU, Glucose Disposal, and EGP

Whole-body GU was assessed by the euglycemic-hyperinsulinemic clamp–based M value and the glucose disposal rate by the ^{18}F-FDG disappearance rate (20). To verify the quality of the euglycemic-hyperinsulinemic clamp, we compared the mean glucose levels during the clamp in p.P50T/*AKT2* carriers and noncarriers; we observed essentially no difference between the two groups (5.0 ± 0.4 and 5.0 ± 0.2 mmol/L, P = 0.53). The rates of whole-body GU (17.6 ± 10.3 vs. 29.2 ± 15.2 μmol/kg/min, P = 0.006) and glucose disposal (25.6 ± 9.9 vs. 33.1 ± 11.9 μmol/kg/min, P = 0.029) were lower in p.P50T/*AKT2* carriers compared with noncarriers (Fig. 1*A*). EGP during the clamp was higher in p.P50T/*AKT2* carriers than in noncarriers (9.0 ± 2.6 vs. 5.8 ± 6.9 μmol/kg/min, P = 0.038).

Tissue-Specific GU

We assessed GU in different tissues using the euglycemic-hyperinsulinemic clamp and PET. We observed lower rates of GU in carriers of the p.P50T/*AKT2* variant compared with noncarriers in skeletal muscle (23.9 ± 14.1 vs. 37.5 ± 20.7 μmol/kg/min, P = 0.012), liver (21.0 ± 5.1 vs. 25.1 ± 6.6 μmol/kg/min, P = 0.030), brown adipose tissue (11.7 ± 5.1 vs. 16.7 ± 6.9 μmol/kg/min, P = 0.004), and bone marrow (13.3 ± 5.4 vs. 19.8 ± 8.8 μmol/kg/min, P = 0.004) (Fig. 1*B* and *C*), but did not observe significant differences in subcutaneous adipose tissue (11.3 ± 4.1 vs. 12.7 ± 5.8 μmol/kg/min, P = 0.488), visceral adipose tissue (17.3 ± 6.4 vs. 20.9 ± 8.5 μmol/kg/min, P = 0.157), myocardium (34.2 ± 16.8 vs. 35.0 ± 12.6 μmol/100 g/min, P = 0.870), duodenum (31.9 ± 7.0 vs. 31.7 ± 7.1 μmol/kg/min, P = 0.931), or jejunum (33.2 ± 7.0 vs. 32.4 ± 7.2 μmol/kg/min, P = 0.711). We observed higher rates of GU in the p.P50T/*AKT2* carriers than in noncarriers in all seven analyzed brain regions (P = 0.001) (Fig. 2).

FFA Levels in Fasting and During the Clamp

Fasting FFA levels did not differ between carriers and noncarriers of p.P50T/*AKT2* (0.43 ± 0.16 vs. 0.39 ± 0.16 mmol/L, P = 0.360). However, FFA levels were higher during hyperinsulinemia at 60 min in carriers than in noncarriers of p.P50T/*AKT2* (0.16 ± 0.12 vs. 0.09 ± 0.05 mmol/L, P = 0.024).

Correlations Between the Rates of Whole-Body and Brain GU With Tissue-Specific GU and EGP in Carriers and Noncarriers of p.P50T/AKT2

The differences in the rates of GU across several tissues between carriers and noncarriers of p.P50T/*AKT2* we observed prompted us to investigate the correlations of the rates of GU separately in carriers and noncarriers of p.P50T/*AKT2*. Whole-body GU correlated positively with skeletal muscle GU (r = 0.92 vs. r = 0.90), bone marrow GU (r = 0.74 vs. r = 0.85), subcutaneous fat GU (r = 0.59 vs. r = 0.40), and liver GU (r = 0.41 vs. r = 0.46), and negatively with brain GU (r = −0.56 vs. r = −0.66) in both noncarriers and carriers of p.P50T/*AKT2*, respectively (Fig. 3*A*). Correlations of the rates of whole-body GU with brown fat GU (r = 0.80 vs. r = 0.36, P = 0.023) and EGP in the liver (r = −0.41 vs. −0.08, P = 0.276) were substantially weaker

Table 1—Clinical and laboratory characteristics of the p.P50T/*AKT2* noncarriers and carriers who participated in the METSIM PET studies

Variable	Noncarriers (N = 25)	Carriers (N = 20)	P value
Age, years	63.9 ± 4.8	61.9 ± 6.3	0.23
Height, cm	176.9 ± 5.3	174.2 ± 5.5	0.10
Weight, kg	87.4 ± 10.2	86.1 ± 11.6.2	0.70
BMI, kg/m^2	28.1 ± 3.4	28.7 ± 3.4	0.60
Waist, cm	100.7 ± 8.9	100.3 ± 8.7	0.88
Fat mass, %	29.0 ± 7.0	28.0 ± 7.0	0.60
Systolic blood pressure, mmHg	133.8 ± 14.1	137.3 ± 15.9	0.44
Diastolic blood pressure, mmHg	86.4 ± 10.1	86.6 ± 8.5	0.94
Fasting plasma glucose, mmol/L	6.0 ± 6.5	6.1 ± 0.3	0.28
Fasting insulin, mU/L	9.4 ± 5.6	17.8 ± 10.2	0.003
LDL cholesterol, mmol/L	3.30 ± 0.96	2.92 ± 1.09	0.21
HDL cholesterol, mmol/L	1.51 ± 0.38	1.33 ± 0.37	0.12
Total triglycerides, mmol/L	1.12 ± 0.50	1.48 ± 1.04	0.26
Alanine transferase, units/L	29.7 ± 13.6	32.6 ± 17.8	0.58
Creatinine, μmol/L	85.3 ± 10.5	85.5 ± 12.6	0.96

Data are mean ± SD. Total triglycerides and alanine transferase were log-transformed to calculate P value.

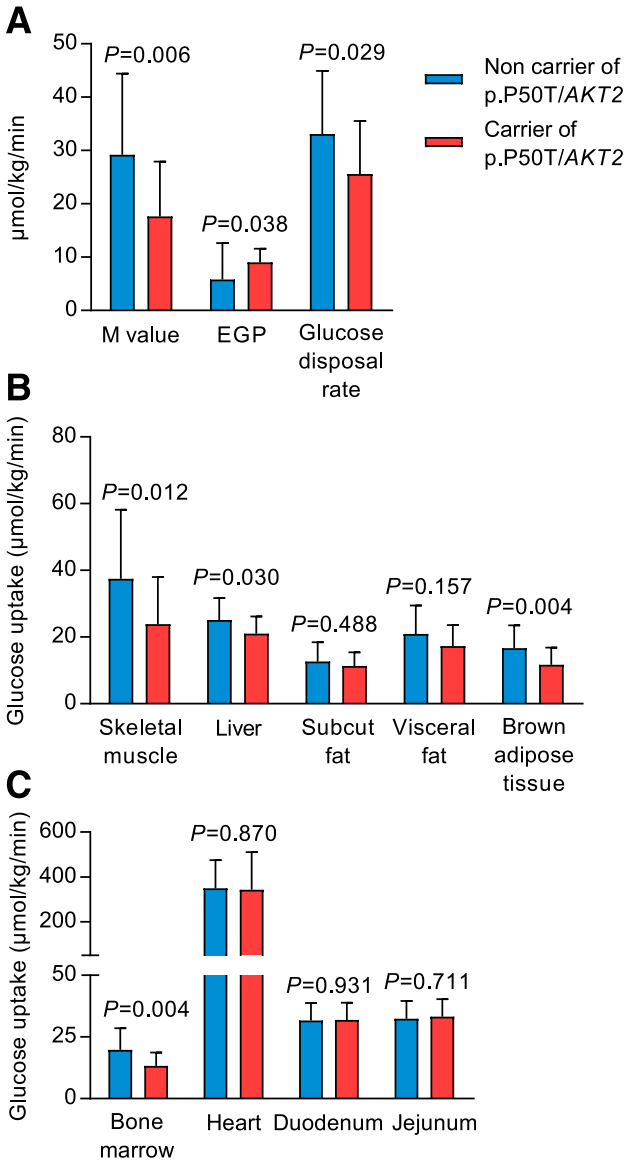

Figure 1—Whole-body and tissue-specific GU. *A*: Whole-body GU (M value), EGP, and whole-body glucose disposal rate in the carriers (red bars, *N* = 20) and noncarriers (blue bars, *N* = 25) of p.P50T/*AKT2*. *B* and *C*: Tissue-specific GU in the carriers (red bars, *N* = 20) and noncarriers (blue bars, *N* = 25) of p.P50T/*AKT2*. Bar heights represent sample means, vertical lines represent sample SDs. *P* values for comparison of carriers versus noncarriers of p.P50T/*AKT2*. Subcut, subcutaneous.

among the carriers than among noncarriers of p.P50T/*AKT2*. Whole-body GU correlated weakly with heart muscle GU and jejunum GU without any substantial difference between the noncarriers and carriers of p.P50T/*AKT2*. Correlations of brain GU with EGP (r = 0.68 vs. r = 0.05, P = 0.016) and bone marrow GU (r = −0.24 vs. r = −0.84, P = 0.002) were significantly different between the noncarriers and carriers of p.P50T/*AKT2* (Fig. 3*B*).

DISCUSSION

Our genotype-based callback PET study demonstrates that a low-frequency partial loss-of-function p.P50T/*AKT2* variant,

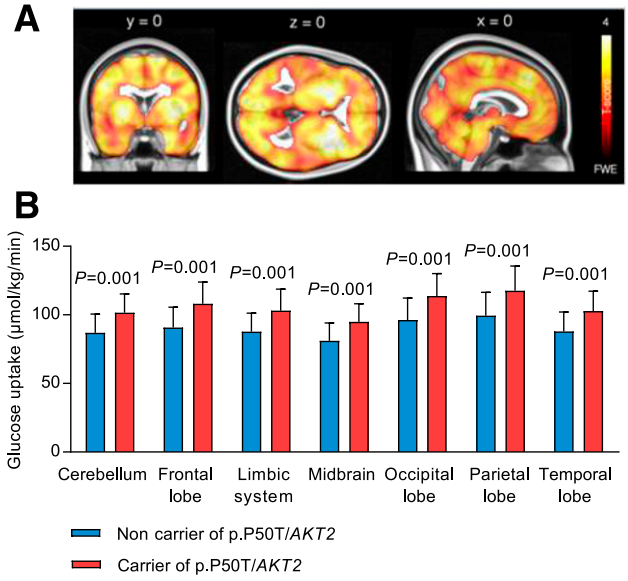

Figure 2—*A*: Brain regions in the PET study where insulin-stimulated GU was measured in carriers and noncarriers of the p.P50T/*AKT2* variant. *B*: Significant differences (*P* value) in GU in the specific regions of the brain between noncarriers (blue bars, *N* = 25) and carriers (red bars, *N* = 20) of the p.P50T/*AKT2* variant. Data are mean ± SD.

nearly unique to Finns and probably originating from a recent bottleneck in the 16th century in the settlement of Eastern Finland (1), is associated with significantly decreased GU in whole body and in multiple insulin-sensitive tissues. This is consistent with our previous study (9) demonstrating that insulin levels were increased in carriers of p.P50T/*AKT2* as a compensatory mechanism for insulin resistance. The increase in insulin levels was substantially less in carriers of p.P50T/*AKT2* compared with carriers of the p.Arg274His/*AKT2* loss-of-function mutation previously reported (6).

Activation of AKT2 is associated with translocation of GLUT4 from intracellular storage vesicles to the cell surface (26,27). AKT2 is the major isoform of AKT and is abundantly expressed in skeletal muscle (8,9). Insulin-stimulated AKT2 activation leads to inactivation of GSK3β (3,28), resulting in increased glycogen synthesis. Moreover, gene silencing experiments have provided evidence that AKT2 is indispensable for insulin action on glucose uptake and glycogen synthesis in human skeletal muscle cells (29). The current study shows that in vivo skeletal muscle GU was reduced by 36% (P = 0.012) in the p.P50T/*AKT2* carriers compared with noncarriers. This could be explained, at least in part, by reduced activity of the low-frequency p.P50T/*AKT2* variant, in agreement with our previous finding of impaired insulin signaling in HeLa cells and human liver HuH7 cells for the variant (9). Collectively, these findings demonstrate that AKT2 is an important determinant of insulin sensitivity in human skeletal muscle.

The liver plays an important role in maintaining normal glucose levels by regulating EGP (gluconeogenesis) and glycogenolysis (glycogen breakdown). Additionally, the kidney

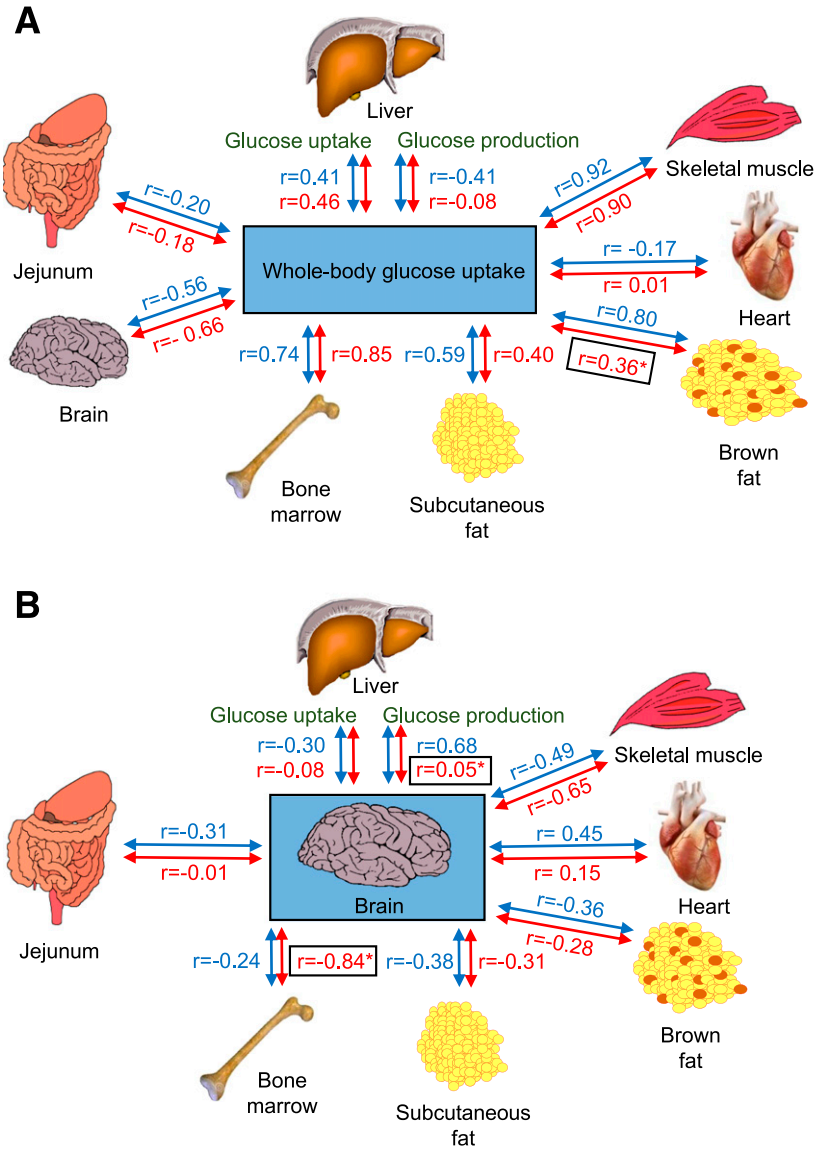

Figure 3—*A*: Correlations of whole-body GU with the tissue-specific GU in skeletal muscle, heart muscle, brown fat, subcutaneous fat, bone marrow, brain, jejunum, and liver in carriers and noncarriers of the p.P50T/*AKT2* variant. *B*: Correlations of the mean brain GU with tissue-specific GU in skeletal muscle, heart muscle, brown fat, subcutaneous fat, bone marrow, jejunum, and liver in carriers and noncarriers of the p.P50T/*AKT2* variant. Blue indicates correlations in noncarriers and red in carriers of the p.P50T/*AKT2* variant. *$P < 0.05$ (exact *P* values are given in the text) for correlations that were significantly different between carriers and noncarriers of the p.P50T/*AKT2* variant.

produces about 20% of EGP (15). Normally, insulin suppresses EGP and inhibits the genes encoding gluconeogenesis and redirects newly synthesized glucose-6-phosphate to glycogen (3). We found that EGP was significantly increased and liver GU decreased in the carriers of the *AKT2* variant compared with noncarriers, indicating liver insulin resistance. AKT2 plays an important role in the regulation of liver and kidney (29) insulin sensitivity. AKT2 phosphorylates and inhibits FOXO1, a key regulator of EGP (30). Our findings agree with the results observed in mice deficient in Akt2, which demonstrated a significant failure of insulin to suppress EGP (2). Additionally, we found that liver GU was decreased in the carriers of the p.P50T/*AKT2* variant compared with noncarriers. This could be due to impaired insulin signaling attributable to the p.P50T/*AKT2* variant, which results in subnormal inactivation of GSK3β. Other mechanisms, independent of GSK3β suppression, could also play a role, as recently suggested (3).

Activation of AKT2 enhances GLUT4 translocation and the rates of GU similarly in adipose tissue and skeletal muscle (6). GU into the white adipose tissue is relatively minor, accounting for only 5–10% of whole-body GU during insulin-stimulated states, suggesting that white adipose tissue does not have a major quantitative role in postprandial glucose metabolism (31,32). We did not find a statistically significant difference between the carriers and noncarriers of p.P50T/*AKT2* in the rates of GU in subcutaneous or visceral adipose tissue, although the rates of GU were slightly

lower in variant carriers than in noncarriers. The carriers and noncarriers of p.P50T/*AKT2* had similar weight, BMI, waist circumference, and fat percentage, making it unlikely that obesity, central obesity, or fat mass could have an effect on the rates of adipose tissue GU. However, we found that the levels of FFAs were higher during the clamp at 60 min in carriers of p.P50T/*AKT2* than in noncarriers, suggesting that insulin's inhibitory effect on adipose tissue lipolysis was impaired in carriers of p.P50T/*AKT2* (33).

Brown adipose tissue is mainly located in the supraclavicular region in adult humans, has high mitochondrial content and insulin sensitivity and rich vasculature, and is activated by cold exposure (34). We observed that the rates of brown adipose tissue GU were significantly lower in p.P50T/*AKT2* variant carriers than in noncarriers, not surprising since hyperinsulinemia increases GU in brown adipose tissue up to fivefold compared with the fasting state (22). A recent study demonstrated that mice lacking adipocyte *Akt1* and *Akt2* had no discernible subcutaneous or brown adipose tissue and developed lipodystrophy, severe insulin resistance, and hepatomegaly (35). However, p.P50T/*AKT2* variant carriers in our study did not have lipodystrophy, reduced fat mass, or elevated liver enzymes (Table 1). This is consistent with our previous in vitro studies showing that p.P50T/*AKT2* is only a partial loss-of-function variant (9). To assess the effects of outside temperature on brown adipose tissue activity, we adjusted statistical analyses for the mean temperatures in the previous 30, 14, and 7 days; these adjustments had no meaningful effect on our results.

Bone marrow of the femoral diaphysis in adults consists mostly of adipocytes. Femoral bone marrow "yellow" adipose tissue, consisting of a moderate number of mitochondria, has intermediate metabolic activity compared with brown and white adipose tissue. It is still unclear whether "yellow" adipose tissue constitutes a homogeneous population of brown or white adipocytes or is a heterogeneous population of both types of adipose tissue cells (36). We have recently shown that femoral bone marrow insulin-stimulated GU correlated with whole-body insulin sensitivity in elderly women (37). Here, we observed a significant correlation of the rates of femoral bone marrow insulin-stimulated GU with the rates of skeletal muscle GU in men. Therefore, it is possible that femoral bone marrow exhibits a similar impairment in GU as skeletal muscle attributable to impaired AKT2 signaling.

Glucose is the major source of energy in the brain. Reduced brain insulin uptake has been postulated to lead to a decrease in brain insulin sensitivity to stimulate central nervous system pathways (38). In a previous PET study, brain GU was similar in participants with impaired glucose tolerance and healthy individuals in the fasting state but increased by 18% during hyperinsulinemia in participants with impaired glucose tolerance and not in healthy participants, suggesting that in insulin-resistant states brain GU is paradoxically increased (39). Similarly, in another PET study, brain GU during hyperinsulinemia was increased in obese but not in nonobese participants (40). In our study, brain GU was greater in p.P50T/*AKT2* variant carriers compared with noncarriers by 16.8–19.1% in different regions of the brain. These results suggest that both acquired (impaired glucose tolerance, obesity) and inherited (p.P50T/*AKT2*) insulin resistance may lead to the increased rates of brain GU. The molecular mechanism of this phenomenon is poorly understood. A recent study in rats demonstrated that ^{18}F-FDG PET signal reflects GU not only in neurons but also in astrocytes (41). Moreover, the insulin signaling cascade is functional in primary human astrocytes and increases Akt serine 473 phosphorylation (42). We plan to investigate the role of p.P50T/*AKT2* in astrocyte GU in in vitro studies.

Interestingly, correlation of brain GU with EGP was significantly different between the noncarriers and carriers of p.P50T/AKT2 (r = 0.68 vs. 0.05, P = 0.016). A previous study in rats demonstrated that hypothalamic insulin signaling has significant effects on liver glucose production during hyperinsulinemia (43). Our results suggest that in p.P50T/*AKT2* carriers, insulin regulation of EGP is lost, resulting in increased glucose production by the liver and kidney during hyperinsulinemia.

The main source of energy in the heart is FFAs, but energy can also be derived from other sources including glucose, pyruvate, and lactate. Therefore, it is not surprising that we did not observe significant differences in myocardial GU between carriers and noncarriers of the p.P50T/*AKT2* variant, in contrast to the substantial differences observed in skeletal muscle. A recent study demonstrated that insulin was able to increase GU by almost threefold in duodenum and jejunum in normal-weight, nonobese participants, but obese participants without diabetes showed no response to insulin, implying insulin insensitivity in the small intestine (23). Although *AKT2* is expressed in small intestine, we did not observe any difference in GU into duodenal or jejunal mucosa between carriers and noncarriers of p.P50T/*AKT2*.

The strengths of our study are a careful matching of the study groups for sex (all male), age, and BMI, strict inclusion criteria to exclude participants with diseases and drug treatments which could have an effect on tissue-specific GU, and the fact that all study procedures at the Turku PET Centre were performed blinded to the genotype of the participants. The tissue-specific differences in the kinetics of ^{18}F-FDG and glucose in skeletal muscle, adipose tissue, liver, and intestine were corrected using lumped constants validated in our laboratory in healthy participants during similar clamp conditions. The primary limitation of the study is that it included only middle-aged and elderly men; it would be interesting to repeat our study in women and younger individuals.

In conclusion, our genotype-based callback study demonstrates a significant decrease of the insulin-mediated GU in skeletal muscle, liver, brown adipose tissue, and bone marrow and an increase of GU in the brain in the carriers of the p.P50T/*AKT2* variant compared with the noncarriers of this variant. These changes in GU may explain, at least in part, the increased risk of type 2 diabetes in p.P50T/*AKT2* carriers. Our study also demonstrates the value of

genotype-based callback studies and the practicality of PET as an informative, noninvasive method to characterize the function of genetic variants of interest.

Acknowledgments. The authors thank the 45 volunteers who participated in this study.

Funding. The authors acknowledge the following funding sources: National Institutes of Health National Heart, Lung, and Blood Institute (NIH/NHLBI 5K01DK107836) (A.K.M.); the Wellcome Trust (095101/Z/10/Z and 200837/Z/16/Z) (A.L.G.); Medical Research Council (MR/L020149/1) (A.L.G.); the Li Ka Shing Foundation (C.M.L.); the National Institute for Health Research Oxford Biomedical Research Centre (C.M.L.); Widenlife (C.M.L.); National Institutes of Health grants CRR00070 CR00.01 (C.M.L.), R01DK093757 (K.L.M.), R01DK072193 (K.L.M.), and U01DK062370 (M.B.); and National Human Genome Research Institute Division of Intramural Research project number Z01HG000024 (F.S.C.). Sequence data were generated by the T2D-GENES Consortium with support from National Institutes of Health National Institute of Diabetes and Digestive and Kidney Diseases grants U01DK085501, U01DK085524, U01DK085526, U01DK085545, and U01DK085584; Suomen Akatemia (Academy of Finland) (321428) (M.L.); Juselius Foundation (M.L.); Sydäntutkimussäätiö (Finnish Foundation for Cardiovascular Research) (M.L.); European Medical Information Framework grant IMI JU GA 115372-2 (M.L.); Kuopion Yliopistollinen Sairaala (Kuopio University Hospital) VTR grant (M.L.); and Centre of Excellence of Cardiovascular and Metabolic Diseases supported by the Academy of Finland (P.N., M.L.). A.L.G. is a Wellcome Trust Senior Fellow in Basic Biomedical Research.

Duality of Interest. No potential conflicts of interest relevant to this article were reported.

Author Contributions. A.L.-R., M.-J.H., A.S., H.A.K., J.K., T.K., L.N., P.N., and M.L. contributed to sample collection and phenotyping. A.K.M., H.S., A.L.G., C.M.L., F.S.C., K.L.M., L.J.S., and M.B. contributed to data production (genotyping). A.L.-R., A.S., L.G., L.J.S., T.K., L.N., M.B., and M.L. contributed to statistical analysis. A.L.-R., M.-J.H., A.S., P.N., and M.L. contributed to study design. L.N., M.B., P.N., and M.L. contributed to study supervision. M.L. is the guarantor of this work and, as such, had full access to all the data in the study and takes responsibility for the integrity of the data and the accuracy of the data analysis.

Prior Presentation. The results were previously presented at the 77th Scientific Sessions of the American Diabetes Association, San Diego, CA, 9–13 June 2017, with the title "A Partial Loss of Function Variant in the AKT2 Gene Is Associated With Reduced Insulin-Mediated Glucose Uptake in Skeletal Muscle, Liver, Brown Adipose Tissue, and Bone Marrow: A Positron Emission Tomography Study" (18-OR).

References

1. Lim ET, Würtz P, Havulinna AS, et al.; Sequencing Initiative Suomi (SISu) Project. Distribution and medical impact of loss-of-function variants in the Finnish founder population. PLoS Genet 2014;10:e1004494

2. Cho H, Mu J, Kim JK, et al. Insulin resistance and a diabetes mellitus-like syndrome in mice lacking the protein kinase Akt2 (PKB beta). Science 2001;292:1728–1731

3. Wan M, Leavens KF, Hunter RW, et al. A noncanonical, GSK3-independent pathway controls postprandial hepatic glycogen deposition. Cell Metab 2013;18:99–105

4. Koren S, DiPilato LM, Emmett MJ, et al. The role of mouse Akt2 in insulin-dependent suppression of adipocyte lipolysis in vivo. Diabetologia 2015;58:1063–1070

5. Garofalo RS, Orena SJ, Rafidi K, et al. Severe diabetes, age-dependent loss of adipose tissue, and mild growth deficiency in mice lacking Akt2/PKB beta. J Clin Invest 2003;112:197–208

6. George S, Rochford JJ, Wolfrum C, et al. A family with severe insulin resistance and diabetes due to a mutation in *AKT2*. Science 2004;304:1325–1328

7. Hussain K, Challis B, Rocha N, et al. An activating mutation of *AKT2* and human hypoglycemia. Science 2011;334:474

8. Gonzalez I, Tripathi G, Carter EJ, et al. Akt2, a novel functional link between p38 mitogen-activated protein kinase and phosphatidylinositol 3-kinase pathways in myogenesis. Mol Cell Biol 2004;24:3607–3622

9. Manning A, Highland HM, Gasser J, et al. A low-frequency inactivating *AKT2* variant enriched in the Finnish population is associated with fasting insulin levels and type 2 diabetes risk. Diabetes 2017;66:2019–2032

10. Stancáková A, Javorský M, Kuulasmaa T, Haffner SM, Kuusisto J, Laakso M. Changes in insulin sensitivity and insulin release in relation to glycemia and glucose tolerance in 6,414 Finnish men. Diabetes 2009;58:1212–1221

11. Laakso M, Kuusisto J, Stančáková A, et al. The Metabolic Syndrome in Men study: a resource for studies of metabolic and cardiovascular diseases. J Lipid Res 2017;58:481–493

12. DeFronzo RA, Tobin JD, Andres R. Glucose clamp technique: a method for quantifying insulin secretion and resistance. Am J Physiol 1979;237:E214–E223

13. Hamacher K, Coenen HH, Stöcklin G. Efficient stereospecific synthesis of no-carrier-added 2-[^{18}F]-fluoro-2-deoxy-D-glucose using aminopolyether supported nucleophilic substitution. J Nucl Med 1986;27:235–238

14. Iozzo P, Gastaldelli A, Järvisalo MJ, et al. ^{18}F-FDG assessment of glucose disposal and production rates during fasting and insulin stimulation: a validation study. J Nucl Med 2006;47:1016–1022

15. Stumvoll M, Meyer C, Mitrakou A, Nadkarni V, Gerich JE. Renal glucose production and utilization: new aspects in humans. Diabetologia 1997;40:749–757

16. Gambhir SS, Schwaiger M, Huang SC, et al. Simple noninvasive quantification method for measuring myocardial glucose utilization in humans employing positron emission tomography and fluorine-18 deoxyglucose. J Nucl Med 1989;30:359–366

17. Patlak CS, Blasberg RG. Graphical evaluation of blood-to-brain transfer constants from multiple-time uptake data. Generalizations. J Cereb Blood Flow Metab 1985;5:584–590

18. Peltoniemi P, Lönnroth P, Laine H, et al. Lumped constant for [(18)F] fluorodeoxyglucose in skeletal muscles of obese and nonobese humans. Am J Physiol Endocrinol Metab 2000;279:E1122–E1130

19. Bøtker HE, Böttcher M, Schmitz O, et al. Glucose uptake and lumped constant variability in normal human hearts determined with [^{18}F]fluorodeoxyglucose. J Nucl Cardiol 1997;4:125–132

20. Iozzo P, Järvisalo MJ, Kiss J, et al. Quantification of liver glucose metabolism by positron emission tomography: validation study in pigs. Gastroenterology 2007;132:531–542

21. Virtanen KA, Peltoniemi P, Marjamäki P, et al. Human adipose tissue glucose uptake determined using [(18)F]-fluoro-deoxy-glucose ([(18)F]FDG) and PET in combination with microdialysis. Diabetologia 2001;44:2171–2179

22. Orava J, Nuutila P, Lidell ME, et al. Different metabolic responses of human brown adipose tissue to activation by cold and insulin. Cell Metab 2011;14:272–279

23. Honka H, Mäkinen J, Hannukainen JC, et al. Validation of [^{18}F]fluorodeoxyglucose and positron emission tomography (PET) for the measurement of intestinal metabolism in pigs, and evidence of intestinal insulin resistance in patients with morbid obesity. Diabetologia 2013;56:893–900

24. Wu HM, Bergsneider M, Glenn TC, et al. Measurement of the global lumped constant for 2-deoxy-2-[^{18}F]fluoro-D-glucose in normal human brain using [^{15}O]-water and 2-deoxy-2-[^{18}F]fluoro-D-glucose positron emission tomography imaging. A method with validation based on multiple methodologies. Mol Imaging Biol 2003;5:32–41

25. Huovinen V, Saunavaara V, Kiviranta R, et al. Vertebral bone marrow glucose uptake is inversely associated with bone marrow fat in diabetic and healthy pigs: [(18)F]FDG-PET and MRI study. Bone 2014;61:33–38

26. Nozaki S, Takeda T, Kitaura T, Takenaka N, Kataoka T, Satoh T. Akt2 regulates Rac1 activity in the insulin-dependent signaling pathway leading to GLUT4 translocation to the plasma membrane in skeletal muscle cells. Cell Signal 2013;25:1361–1371

27. Calera MR, Martinez C, Liu H, Jack AK, Birnbaum MJ, Pilch PF. Insulin increases the association of Akt-2 with Glut4-containing vesicles. J Biol Chem 1998;273:7201–7204

28. Cross DA, Alessi DR, Cohen P, Andjelkovich M, Hemmings BA. Inhibition of glycogen synthase kinase-3 by insulin mediated by protein kinase B. Nature 1995; 378:785–789
29. Bouzakri K, Zachrisson A, Al-Khalili L, et al. siRNA-based gene silencing reveals specialized roles of IRS-1/Akt2 and IRS-2/Akt1 in glucose and lipid metabolism in human skeletal muscle. Cell Metab 2006;4:89–96
30. Sasaki M, Sasako T, Kubota N, et al. Dual regulation of gluconeogenesis by insulin and glucose in the proximal tubules of the kidney. Diabetes 2017;66: 2339–2350
31. Sharabi K, Tavares CD, Rines AK, Puigserver P. Molecular pathophysiology of hepatic glucose production. Mol Aspects Med 2015;46:21–33
32. Virtanen KA, Lönnroth P, Parkkola R, et al. Glucose uptake and perfusion in subcutaneous and visceral adipose tissue during insulin stimulation in nonobese and obese humans. J Clin Endocrinol Metab 2002;87:3902–3910
33. Berggreen C, Gormand A, Omar B, Degerman E, Göransson O. Protein kinase B activity is required for the effects of insulin on lipid metabolism in adipocytes. Am J Physiol Endocrinol Metab 2009;296:E635–E646
34. Virtanen KA, Lidell ME, Orava J, et al. Functional brown adipose tissue in healthy adults. N Engl J Med 2009;360:1518–1525
35. Shearin AL, Monks BR, Seale P, Birnbaum MJ. Lack of AKT in adipocytes causes severe lipodystrophy. Mol Metab 2016;5:472–479
36. Krings A, Rahman S, Huang S, Lu Y, Czernik PJ, Lecka-Czernik B. Bone marrow fat has brown adipose tissue characteristics, which are attenuated with aging and diabetes. Bone 2012;50:546–552
37. Huovinen V, Bucci M, Lipponen H, et al. Femoral bone marrow insulin sensitivity is increased by resistance training in elderly female offspring of overweight and obese mothers. PLoS One 2016;11:e0163723
38. Kullmann S, Heni M, Hallschmid M, Fritsche A, Preissl H, Häring HU. Brain insulin resistance at the crossroads of metabolic and cognitive disorders in humans. Physiol Rev 2016;96:1169–1209
39. Hirvonen J, Virtanen KA, Nummenmaa L, et al. Effects of insulin on brain glucose metabolism in impaired glucose tolerance. Diabetes 2011;60:443–447
40. Tuulari JJ, Karlsson HK, Hirvonen J, et al. Weight loss after bariatric surgery reverses insulin-induced increases in brain glucose metabolism of the morbidly obese [published correction appears in Diabetes 2017;66:2724]. Diabetes 2013;62: 2747–2751
41. Zimmer ER, Parent MJ, Souza DG, et al. [^{18}F]FDG PET signal is driven by astroglial glutamate transport. Nat Neurosci 2017;20:393–395
42. Heni M, Hennige AM, Peter A, et al. Insulin promotes glycogen storage and cell proliferation in primary human astrocytes. PLoS One 2011;6:e21594
43. Obici S, Zhang BB, Karkanias G, Rossetti L. Hypothalamic insulin signaling is required for inhibition of glucose production. Nat Med 2002;8:1376–1382